


Reduced sensitivity to disorder in a coupled-resonator waveguide with disordered coupling coefficients

Rujiang Li  and Yakir Hadad 

School of Electrical Engineering, Tel-Aviv University, Ramat-Aviv, Tel-Aviv 69978, Israel



(Received 1 March 2020; accepted 22 January 2021; published 5 February 2021)

Disorder and structural imperfections are unavoidable and challenge wave engineering. Therefore, methods to reduce disorder and its effects are persistently sought for. Here, we theoretically explore a kind of a bulk mode that is supported by a periodic coupled resonator waveguide with odd length. Although it is a bulk mode, its eigenfrequency is unaffected by disorder, and furthermore, its corresponding eigenvector is stationary under the influence of moderate disorder. Therefore, as we prove analytically and demonstrate numerically, the resonant transmission near its eigenfrequency exhibits substantially reduced sensitivity to disorder compared to any other frequency in the passband.

DOI: [10.1103/PhysRevA.103.023503](https://doi.org/10.1103/PhysRevA.103.023503)

I. INTRODUCTION

Disorder is unavoidable in any analog system, either natural or manmade, due to impurities, structural defects, and fabrication tolerances which imply the precision at which the system may be implemented. An important consequence of disorder is reduced diffusion and mode localization that were originally introduced by Anderson [1] for electronic lattices with on-site disordered potential. However, Anderson localization is a much broader wave phenomenon that applies to any kind of wave system that exhibits disorder, either photonic [2–7], acoustic [8,9], elastic [10], etc. Active research on disorder in discrete one-dimensional (1D) lattices has been carried out already before Anderson’s work. Dyson [11] explored analytical solutions for the dynamics of disordered 1D lattices in what he coined as the “one-dimensional glass” model. Following Dyson, additional aspects of disordered 1D crystals have been studied by several authors [12–16].

Occasionally, localization is considered as a desired property, e.g., for random lasing [17,18] or even, surprisingly, to induce protected edge states [19,20]. However, typically, it is regarded as a challenge since it leads to reduced transport. Therefore, venues to overcome the effect of disorder, as well as scenarios in which it has weaker influence, are constantly sought.

Mode localization, and thereby reduced transport, is a consequence of the coupling between a degenerate pair of counterpropagating waves along a scattering path. Therefore, systems with broken time-reversal symmetry are considered useful to reduce the localization effect as they revoke the underlying physics behind it. These include strongly nonreciprocal systems such as one-way guiding structures [21–27] and topologically protected systems with broken time-reversal symmetry [28–31]. However, breaking time-reversal symmetry is not a trivial task as it requires the application of external

biasing, such as static magnetization [21–23], space-time modulation [24,25,32], or motion [26,27,33]. Therefore, it is interesting to seek for systems that are time-reversal but yet exhibit weaker effect by the presence of disorder. Thus, in this paper we explore the transmission through one-dimensional, time-reversal, coupled resonator waveguides with disorder present in their coupling coefficients.

One dimensional lattices with disordered off-diagonal coupling coefficients have been studied for decades already. They were first introduced as the “Case I” disorder in Dyson’s work [11] and later explored in the context of the one-dimensional XY model [34]. In photonics, Anderson localization in optical waveguides with off-diagonal coupling disorder has been shown in Ref. [6]. Interestingly, it has been argued that the zero-energy (*midband*) state is delocalized regardless of the probability distribution of the coupling coefficients [35], and their density of states at that energy vicinity is singular [36]. Nevertheless, Soukoulis and Economou [37] have established that, although the localization length of the zero-energy state diverges at infinity, it should yet be considered as localized since the transmission coefficient approaches zero as the size of the system approaches infinity. Leaving aside the infinite lattice, for a finite lattice, by calculating the Landauer conductance of electrons, the delocalization effect at the midband energy has been shown to be present if and only if the lattice size is odd [38], and the density of states at that center energy exhibits significantly different behavior for odd and even lattice lengths [39].

In recent years the topologically protected zero-frequency (*midgap*) edge modes of the dimer lattice, the Su-Schreifer-Heeger (SSH) model, have been suggested for disorder immune analog signal processing [40] and have been shown to be robust also in terms of input impedance [41]. In contrast to the use of topologically protected disorder immune edge modes, and in accord with Refs. [38,39], in this paper we revisit the problem of resonant wave transmission through a finite lattice with disordered coupling coefficients, this time based on a *bulk mode*. As a case study we focus on the

*hadady@eng.tau.ac.il

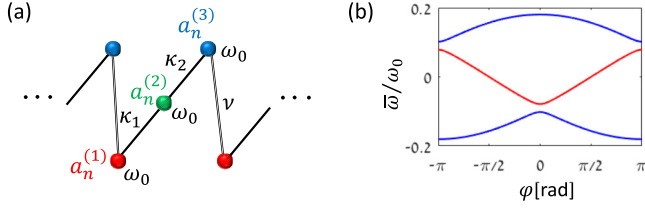


FIG. 1. (a) Unit cell of the trimer lattice. (b) Typical dispersion for $\kappa_1 = 0.1\omega_0$, $\kappa_2 = 0.08\omega_0$, and $\nu = 0.09\omega_0$.

trimerized unit-cell lattice, and we calculate the transmission between two wave ports that are connected at the edges of the lattice. We express the transmission in the disordered lattice and show that the transmission at a narrow frequency band about the passband midfrequency is stationary with respect to substantial disorder. Moreover, we study numerically by Monte Carlo simulations the robustness of the wave transmission through the lattice and explore not only the magnitude of the transmission coefficient but also the group delay, which is important in the context of disorder immune optical and acoustic coupled resonator waveguides.

II. THE TRIMERIZED LATTICE

We explore the transmission through a coupled resonator lattice with trimerized unit cells as illustrated in Fig. 1(a). Each unit cell in the lattice consists of three identical resonators, resonating at ω_0 , bonded by two intracell coupling coefficients, κ_1 and κ_2 , and one intercell coupling coefficient, ν . The lattice dynamics obeys the following:

$$i\dot{a}_n^{(1)} = \omega_0 a_n^{(1)} + \kappa_1 a_n^{(2)} + \nu a_{n-1}^{(3)}, \quad (1a)$$

$$i\dot{a}_n^{(2)} = \omega_0 a_n^{(2)} + \kappa_1 a_n^{(1)} + \kappa_2 a_n^{(3)}, \quad (1b)$$

$$i\dot{a}_n^{(3)} = \omega_0 a_n^{(3)} + \kappa_2 a_n^{(2)} + \nu a_{n+1}^{(1)}, \quad (1c)$$

where $a_n^{(j)}(t)$ denotes the mode amplitude of the j th resonator in the n th unit cell, and $\dot{a}_n^{(j)}(t) = da_n^{(j)}/dt$. See, e.g., Ref. [42] for electronic circuit implementation of a similar model. The dispersion of the lattice guided modes is derived in Appendix A and a typical dispersion diagram is shown in Fig. 1(b) for $\kappa_1 = 0.1\omega_0$, $\kappa_2 = 0.08\omega_0$, and $\nu = 0.09\omega_0$. In Fig. 1, φ stands for the Floquet-Bloch phase, and $\bar{\omega} = \omega - \omega_0$ is the tuned radial frequency about the resonance frequency of an isolated resonator. The trimer lattice is particularly interesting as it gives rise to various modal properties. It may be inversion symmetric when two of the three coupling coefficients are identical, e.g., $\kappa_1 = \kappa_2 \neq \nu$. In that case it can be either topologically trivial, supporting no edge modes, or topologically nontrivial, supporting four edge modes, two at each edge. However, for the general case $\kappa_1 \neq \kappa_2 \neq \nu$, due to its broken inversion symmetry, integer topological numbers cannot be associated with its band structure [43] (see also Appendix B). And therefore, as opposed to the SSH model, the bulk-boundary correspondence [44,45] becomes invalid, where the edge states in the inversion-symmetry broken phase only appear at a single edge. This implies that the idea of topological protection in this system is in general indirect, if applicable at all. Nevertheless, these chiral edge states still

remain relatively robust to substantial disorder [46]. However, as in the SSH model, their exponential nature imposes challenges on their practical use.

A. Disorder insensitive bulk mode

For a finite trimer lattice with N unit cells, Eq. (1) can be used to write the system's Hamiltonian, \mathcal{H} , as a tridiagonal $3N \times 3N$ matrix. Consider the eigenvalue problem $\mathcal{H}\mathbf{x}_j = \bar{\omega}_j \mathbf{x}_j$ with eigenvalues $\bar{\omega}_j$ and eigenvectors \mathbf{x}_j ($j \in [1, 3N]$). The eigenvalues may be found by solving $\det(\mathcal{H} - \bar{\omega}\mathcal{I}) = 0$, where \mathcal{I} denotes the $3N \times 3N$ identity matrix. In this case the determinant can be easily calculated using the recurrence formula $f_j = \bar{\omega}f_{j-1} - b_{j-1}c_{j-1}f_{j-2}$, where $f_{-1} = 0$, $f_0 = 1$, and $f_1 = \bar{\omega}$. Here, b_j and c_j denote the elements on the first sub- and superdiagonals, respectively. Moreover, $b_j = c_j$ as can be easily verified by the requirements for time reversibility and energy conservation [47]. For the ordered lattice $\{b_j\} = \{\dots, \kappa_1, \kappa_2, \nu, \kappa_1, \dots\}$. Since we have N trimerized unit cells, $\det(\mathcal{H} - \bar{\omega}\mathcal{I}) = f_{3N}$. In light of the recursion formula above, clearly, $f_j \sim \bar{\omega}$ for any odd j . Therefore if the lattice consists of an odd number of unit cells it is certain that there exists a mode, say with index $j = m$, with zero eigenvalue $\bar{\omega}_m = 0$ [48]. In the following, this mode is termed the zero-frequency-mode. Note that the eigenvalue $\bar{\omega}_m = 0$ exists regardless of the actual values of the Hamiltonian off-diagonal terms b_j and c_j . Consequently, it remains an eigenvalue in the presence of any disorder in the lattice coupling coefficients. In the following we show that the eigenvalue robustness implies weaker sensitivity of the corresponding eigenvector and thereby of the transmission about that frequency. To that end we employ eigenvalue perturbation theory. We stress that here we do not follow the typical perturbation theory analysis which starts by postulating the invariance of the eigenvector under perturbation in order to evaluate the effect on the corresponding eigenvalue. Here, instead, as a mathematical fact we know, as we discuss above, that the m th eigenvalue is invariant under the influence of disorder, and we seek to find the effect on the eigenvector.

Resorting to the theory of eigenvalue perturbation [49], let us denote by $\hat{\mathcal{H}}$ the perfect lattice Hamiltonian and by $\delta\mathcal{H}$ an additive random perturbation that is caused by disorder in the lattice's coupling coefficients. Under the definitions above, the Hamiltonian of the disordered lattice reads $\mathcal{H} = \hat{\mathcal{H}} + \delta\mathcal{H}$. Assuming that the eigenvalues and eigenvectors of the unperturbed Hamiltonian $\hat{\mathcal{H}}$ are denoted by an "over-hat," $\hat{\omega}_j$ and $\hat{\mathbf{x}}_j$. Then, for the distorted system \mathcal{H} , up to the first order in $\delta\mathcal{H}$ we may approximate the eigenvalues as

$$\bar{\omega}_j \approx \hat{\omega}_j + \hat{\mathbf{x}}_j^T \delta\mathcal{H} \hat{\mathbf{x}}_j \quad (2)$$

and their corresponding eigenvectors as

$$\mathbf{x}_j \approx \hat{\mathbf{x}}_j + \sum_{k \neq j} \frac{[\hat{\mathbf{x}}_k^T \delta\mathcal{H} \hat{\mathbf{x}}_j / (\hat{\omega}_j - \hat{\omega}_k)]}{\hat{\omega}_j - \hat{\omega}_k} \hat{\mathbf{x}}_k. \quad (3)$$

Equation (2) and (3) apply for any mode of the disordered lattice. In particular, for the zero-frequency mode, Eq. (2) implies that $\hat{\mathbf{x}}_m^T \delta\mathcal{H} \hat{\mathbf{x}}_m = 0$. Since $\mathbf{x}_m \neq \mathbf{0}$ and $\delta\mathcal{H}$ is not a rotation matrix, we conclude that \mathbf{x}_m has to belong to the null-space of $\delta\mathcal{H}$, namely, $\delta\mathcal{H}\hat{\mathbf{x}}_m = \mathbf{0}$, where $\mathbf{0}$ denotes the $1 \times 3N$ zero vector (see also Appendix C). Applying Eq. (3), we obtain that

zero-frequency eigenvector is stationary under the influence of disorder, i.e.,

$$\mathbf{x}_m = \hat{\mathbf{x}}_m + O(\delta H^2), \quad (4)$$

as opposed to any other mode of the lattice. We should be careful here and stress that this result is based on a first-order derivation in $\delta\mathcal{H}$, and therefore, as the perturbation increases too much, the effect on the zero-frequency eigenvector will increase as well. Yet, it is clear now that the zero-frequency eigenvector is substantially less sensitive to lattice disorder compare to any other mode—including the supported localized edge modes.

B. Transmission with reduced sensitivity to disorder

Up to this point we have considered only the influence of disorder over the modal properties of the lattice. In the following we study the transmission through a disordered trimerized lattice using the Green's function approach. For the transmission problem, the coupled mode equations for the source-free system in Eq. (1) should be modified to include the input and output ports. To that end, the equations for the first and last resonators in the lattice are rewritten as

$$i\dot{a}_1^{(1)} = (\omega_0 - i\gamma)a_1^{(1)} + \kappa_1 a_1^{(2)} + idS_{\text{in}}, \quad (5)$$

$$i\dot{a}_N^{(3)} = (\omega_0 - i\gamma)a_N^{(3)} + \kappa_2 a_N^{(2)}, \quad (6)$$

where γ is the decay rate induced by the coupling with the input or output port [47], $d = \sqrt{2\gamma}$ is the coupling coefficient between the resonator and the input or output port [50], and $S_{\text{in}} = S_0 \exp(-i\omega t)$ is the input signal with amplitude S_0 and radial frequency ω . Since the excitation is time harmonic and the system is linear and time invariant, the steady state response will be also harmonic and at the same frequency. Therefore, it is convenient to associate each time-harmonic signal at frequency ω to a complex amplitude denoted by a tilde. Thus, for the incoming signal we have $\tilde{S}_{\text{in}} = S_0$. Following this notation we use $\tilde{\mathbf{a}} = [\tilde{a}_1^{(1)}, \tilde{a}_1^{(2)}, \dots, \tilde{a}_N^{(2)}, \tilde{a}_N^{(3)}]^T$ for the complex amplitude of all the resonators in the lattice. We moreover define the input signal vector as $\tilde{\mathbf{S}}_{\text{in}} = S_0 \mathbf{W}_{\text{in}}^T$, where $\mathbf{W}_{\text{in}}^T = [1, 0, 0, \dots, 0]$ is a $1 \times 3N$ vector. Then, the resulting complex mode amplitudes are found by solving the linear system

$$(\mathcal{I}\bar{\omega} - i\gamma\mathcal{U} - \mathcal{H})\tilde{\mathbf{a}} = id\tilde{\mathbf{S}}_{\text{in}}. \quad (7)$$

Here, $\mathcal{U} = \text{diag}\{1, 0, 0, \dots, 0, 1\}$ is a $3N \times 3N$ diagonal matrix that we use in order to include the complex resonance frequencies at the first and last resonators. Once found, $\tilde{\mathbf{a}}$ is used to calculate the output signal $\tilde{S}_{\text{out}} = d\tilde{a}_N^{(3)}$ and the *complex amplitude transmittance*

$$\mathcal{T}(\bar{\omega}) = \tilde{S}_{\text{out}}/\tilde{S}_{\text{in}}, \quad (8)$$

from which the *power transmittance* $T(\bar{\omega}) = |\mathcal{T}(\bar{\omega})|^2$ and the *group delay* $\tau_g(\bar{\omega}) = d \arg[\mathcal{T}(\bar{\omega})]/d\bar{\omega}$ are found. In order to solve Eq. (7) for the complex amplitudes $\tilde{\mathbf{a}}$ we first expand the input vector $\tilde{\mathbf{S}}_{\text{in}}$ in terms of the eigenvectors of $\mathcal{H} + i\gamma\mathcal{U}$, denoted here with \mathbf{x}_j . Thus, $\tilde{\mathbf{S}}_{\text{in}} = \sum_j (\mathbf{x}_j^T \tilde{\mathbf{S}}_{\text{in}}) \mathbf{x}_j$, and conse-

quently we may write

$$\tilde{\mathbf{a}} = \sum_j [id(\mathbf{x}_j^T \tilde{\mathbf{S}}_{\text{in}})/(\bar{\omega} - \bar{\omega}_j)] \mathbf{x}_j, \quad (9)$$

where $\bar{\omega}_j$ is the resonance frequency of the j th mode. The resonance frequencies of the lattice with the two ports become complex due to the out-coupling terms γ . They are given by Eq. (2), with $\delta\mathcal{H} \mapsto \delta\mathcal{H} - i\gamma\mathcal{U}$, as

$$\bar{\omega}_j \approx \hat{\omega}_j + \hat{\mathbf{x}}_j^T \delta\mathcal{H} \hat{\mathbf{x}}_j - i\gamma \hat{\mathbf{x}}_j^T \mathcal{U} \hat{\mathbf{x}}_j, \quad (10)$$

and similarly the eigenvectors are given by Eq. (3) as

$$\mathbf{x}_j \approx \hat{\mathbf{x}}_j + \sum_{k \neq j} \frac{\hat{\mathbf{x}}_k^T \delta\mathcal{H} \hat{\mathbf{x}}_j}{\hat{\omega}_j - \hat{\omega}_k} \hat{\mathbf{x}}_k - i\gamma \sum_{k \neq j} \frac{\hat{\mathbf{x}}_k^T \mathcal{U} \hat{\mathbf{x}}_j}{\hat{\omega}_j - \hat{\omega}_k} \hat{\mathbf{x}}_k. \quad (11)$$

The transmitted wave is given by $\tilde{S}_{\text{out}} = d\tilde{a}_N^{(3)} = d\mathbf{W}_{\text{out}}^T \tilde{\mathbf{a}}$, where $\mathbf{W}_{\text{out}}^T = [0, 0, \dots, 0, 1]$ is a $1 \times 3N$ vector. Substitution in Eq. (8) yields the complex amplitude transmittance between the two ports $\mathcal{T}(\bar{\omega}) = d\mathbf{W}_{\text{out}}^T \tilde{\mathbf{a}}/S_0$. Using Eq. (9), near the j th resonance we may approximate

$$\mathcal{T} \approx d^2 (\mathbf{x}_j^T \mathbf{W}_{\text{in}}) (\mathbf{W}_{\text{out}}^T \mathbf{x}_j) / (\bar{\omega} - \bar{\omega}_j), \quad (12)$$

where ω_j and \mathbf{x}_j are given in Eqs. (10) and (11). However, specifically, near the resonance frequency of the zero-frequency mode, and up to the first order in the disorder $\delta\mathcal{H}$, the transmission reads

$$\mathcal{T} \approx \frac{d^2 (\hat{\mathbf{x}}_m^T \mathbf{W}_{\text{in}}) (\mathbf{W}_{\text{out}}^T \hat{\mathbf{x}}_m)}{\bar{\omega} - \hat{\omega}_m - i\gamma \hat{\mathbf{x}}_m^T \mathcal{U} \hat{\mathbf{x}}_m}, \quad (13)$$

where $\hat{\omega}_m = 0$ and $\hat{\mathbf{x}}_m$ is given by Eq. (4). Equation (13) is a key result of this paper as it clearly shows that, as opposed to any other frequency range within the passband, the disorder effect on the transmission near $\bar{\omega} = 0$ is not $O(\delta\mathcal{H})$ but at least $O(\delta\mathcal{H}^2)$. Implying that the transmission at the narrow band about the zero frequency is substantially persistent against lattice disorder in the coupling coefficients.

C. Monte-Carlo study of transmission

In the following we validate our analytical conclusions and explore their limitations. We consider a finite lattice with $N = 19$ trimerized unit cells. We use $\omega_0 = 1$ as the normalized resonance frequency of each resonator, and $\hat{\kappa}_1 = 0.1$, $\hat{\kappa}_2 = 0.08$, and $\hat{\nu} = 0.09$ for the intracell and intercell coupling coefficients, respectively. As before the ‘‘over-hat’’ is used to denote nominal values of the perfect lattice only. The lattice is connected via two ports, input and output, as discussed above, with $\gamma = 0.01$. See Fig. 2(a) for illustration. The excitation is time harmonic with frequency ω and thus we solve Eq. (7) and use Eq. (8) to derive the complex amplitude transmittance $\mathcal{T}(\bar{\omega})$ from which the power transmittance $T(\bar{\omega})$ and the group delay $\tau_g(\bar{\omega})$ are obtained as given after Eq. (8). Figure 2(b) shows the power transmittance spectrum for the perfect lattice case. In particular we zoom in around $\bar{\omega} = 0$ to highlight the zero-frequency transmission peak, marked by ω_0 , and the next-neighbor peak marked by ω_1 . In the following we turn to explore the transmittance behavior under the influence of disorder in the coupling coefficients. To be specific, we compare between the performance about the zero-frequency ω_0 peak and about the next-neighbor peak ω_1 . The latter is selected

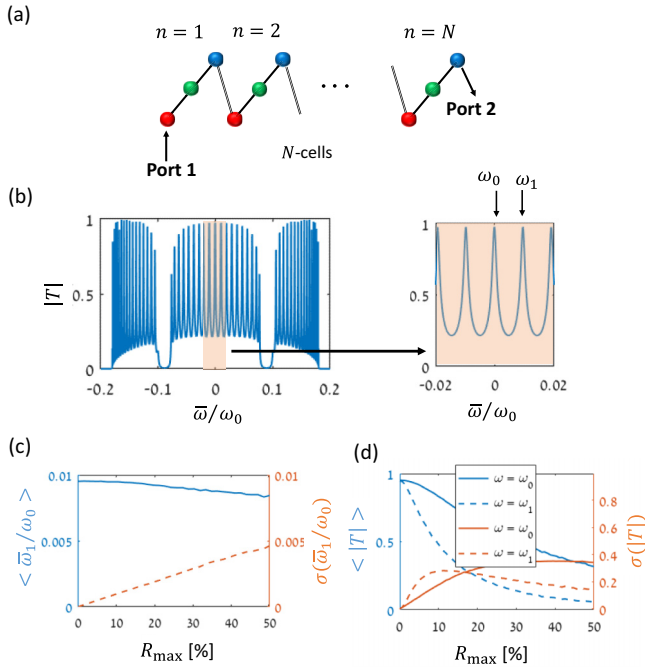


FIG. 2. (a) Illustration of a finite, N -cell chain with input and output ports, #1 and #2. (b) Typical transmission spectra with the parameters for Fig. 1(b) and with $\gamma = 0.01$. Inset on the right: Zoom in of the first few transmission peaks. (c) In the presence of disorder to the coupling coefficients, the location of the zero frequency bulk mode peak is persistent. As opposed to that, the mean and standard deviation of the next transmission peak are shown to be strongly affected. $2 \times R_{\max}$ denotes the assumed tolerance on the coupling elements. (d) Average and standard deviation of transmission at the zero frequency and at the next peak. Illustrating substantial persistence of the zero-frequency mode also in transmission.

as it provides a typical behavior outside the zero-frequency narrow range. For this study, on top of the nominal coupling coefficients of the perfect lattice, we introduce, for each unit cell and at each coupling bond, some random amount of disorder that is uniformly distributed. That is,

$$C_n = \hat{C}(1 + R_{\max}U[-1, 1]), \quad (14)$$

where C stands for either κ_1 , κ_2 or ν at the unit-cell number n , $U[-1, 1]$ denotes a uniform distribution function between -1 and 1 , R_{\max} denotes the allowed tolerance, and “over-hat,” as before, is used to denote nominal value. Recalling the discussion preceding Eq. (2), the zero-frequency resonance frequency is not affected by any level of disorder to the coupling coefficients. As opposed to that, in Fig. 2(c) we see the mean value and the standard deviation of the next peak ω_1 as a function of the tolerance R_{\max} . These statistics have been obtained using repeated *two million* numerical experiments. Comparison between the power transmittance, mean value and standard deviation, is shown in Fig. 2(d). It is evident that the transmittance mean value at the persistent zero-frequency peak is much larger than the standard deviation, as well as larger than the mean value at ω_1 for tolerances below $\sim \pm 25\%$. Nevertheless, one may argue that the mean value and standard deviation are insufficient to predict the likelihood that the transmittance will be above a certain quality. To address this

issue, in Fig. 3 we explore the probability density function (PDF) of the power transmittance and the group delay for the trimerized lattice at ω_0 and ω_1 , and we compare to the transmission performance of a topologically protected SSH edge mode. As a reference, in Figs. 3(a) and 3(b) we show, for very low tolerance, $R_{\max} = 1\%$, the PDF of the power transmittance and group delay at ω_0 and ω_1 . Clearly, in the presence of such a weak disorder, the transmission properties are nearly identical at ω_0 and ω_1 . However, as soon as the tolerance parameter R_{\max} increases to 5%, 10% and 20%, the performance at the ω_1 peak significantly deteriorates as demonstrated in Figs. 3(c). Specifically, already with $R_{\max} = 5\%$ substantial spread of the power transmittance PDF is evident. With moderate (10%) and high (20%) tolerances, it becomes more likely to have, at ω_1 , power transmission that is closer to zero than to unity. In these cases, the group delay distribution significantly deviates from the nearly perfect lattice case as shown in Fig. 3(d). As opposed to that, as shown in Fig. 3(e), the power transmittance at ω_0 remains highly localized near $|T| = 1$ for $R_{\max} = 5\%$ and 10% [compare with Fig. 3(a)], and moderate deviation begins to take effect with $R_{\max} = 20\%$. Moreover, while the group delay PDFs experience moderate spreading as shown in Fig. 3(f), they maintain their mean value compared to Fig. 3(b) and remain localized compared to Fig. 3(d). Interestingly, the persistence to disorder that is demonstrated with the zero-frequency resonance in the one-dimensional trimerized lattice reminds us of the robustness of the topologically protected gap modes in the SSH model. In order to enable a quantitative comparison, in Figs. 3(g) and 3(h) we show the power transmittance and group delay PDFs that are obtained at the edge mode resonance of a SSH lattice $\omega = \omega_{\text{EM}}$. To make a fair comparison, we use for the calculation a SSH lattice with 56 resonators (as opposed to 57 in the trimerized case), each resonates at $\omega = \omega_0$. The resonators are bonded with intercell and intracell coupling coefficients, $\kappa = 0.1$ and $\nu = 0.09$, respectively. This choice of parameters keeps similar the frequency spacing between the resonances in the SSH model and in the trimerized lattice model. Using these parameters the edge mode resonances satisfy $\omega_{\text{EM}} \approx \omega_0$. Moreover, due to “radiation loss” caused by the lattice wave ports ($\gamma = 0.01$) the edge mode transmission using the selected SSH model parameters and length is about $T = 0.65$ in the perfect lattice. Figure 3(g) reveals that the power transmittance distribution is significantly affected even by the presence of low tolerance $R_{\max} = 5\%$; as the tolerance increases, the performance deteriorates further. Compare with Fig. 3(e). Interestingly, however, the group delay performance remains relatively stable as shown in Fig. 3(h).

III. CONCLUSIONS

In this paper we have explored the resonant transmission based on the zero-frequency bulk mode in a periodic lattice with odd length and showed its high persistency against disorder that is present in the lattice bonds. While the *disorder immunity* shares similar characteristics with what is expected by a topologically protected 1D lattice such as the SSH model (see Fig. 3), the underlying physics is completely distinct. The SSH lattice has been suggested recently for disorder immune analog signal processing [40] and has been shown to be robust

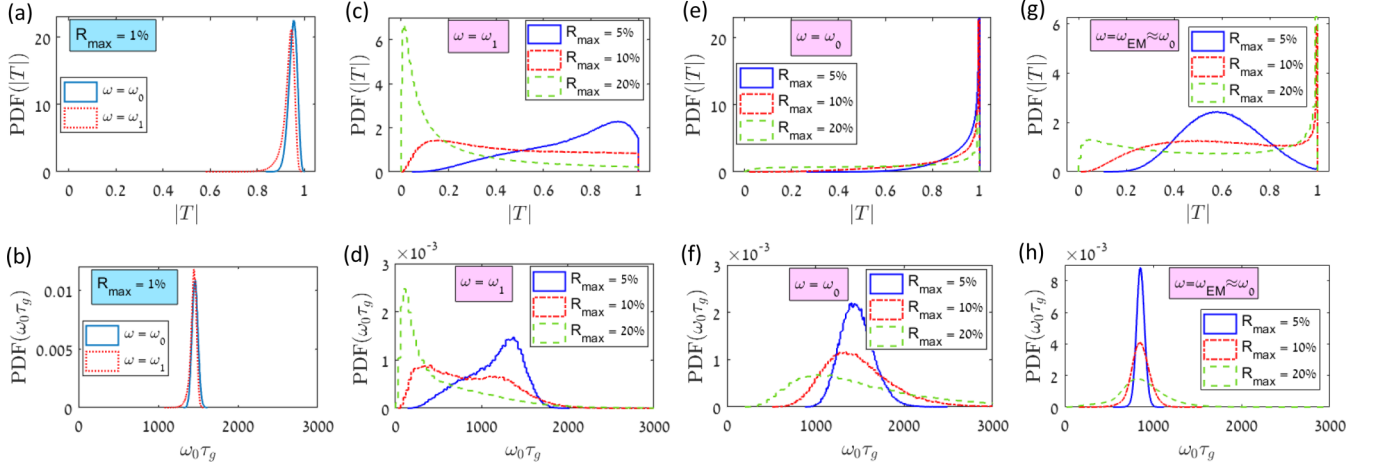


FIG. 3. Study of the probability density function (PDF) for the power transmission and group delays. (a) Power transmittance at ω_0 and ω_0 with low tolerance $R_{\max} = 1\%$. (b) Same as in panel (a) but for the group delay. (c, d) Power transmittance and group delay for the trimerized lattice at a typical bulk mode resonance $\omega = \omega_1$. PDF curves are shown for moderate (5% and 10%) and for high (20%) tolerances. (e, f) Same as in panels (c) and (d) but at the zero-frequency resonance $\omega = \omega_0$. Substantial persistency is evident by the localization of the PDF curves. (g, h) Same as in panels (c) and (d) but for a SSH lattice with parameters given in the text.

also in terms of input impedance [41]. Thus we suggest the plausibility to have similar potential applications using, instead, a topologically trivial bulk mode that exhibits disorder immunity. Last, we point out that, in light of the generality of the model discussed, this kind of disorder immune transmission may be realizable in structures implemented using electronic circuits [41], coupled acoustic resonators [40], and photonic crystals [29].

ACKNOWLEDGMENTS

Y.H. acknowledges support by the Alon Fellowship granted by the Israeli Council of Higher Education (2018-2020). Y.H. thanks Professor Tirza Routtenberg and Dr. Yarden Mazor for useful discussions.

APPENDIX A: BAND STRUCTURE TRIMERIZED LATTICE

Assuming Bloch-wave solution $a_n^{(j)} = e^{in\varphi}$, $j = 1, 2$, and 3, in the coupled mode model Eq. (1), the following dispersion relation is obtained,

$$\bar{\omega}^3 - (\kappa_1^2 + \kappa_2^2 + \nu^2)\bar{\omega} - 2\kappa_1\kappa_2\nu \cos \varphi = 0. \quad (\text{A1})$$

Upon solving it, we get three solutions:

$$\bar{\omega}_1 = A_+^{1/3} + A_-^{1/3}, \quad (\text{A2})$$

$$\bar{\omega}_2 = \bar{\omega}_{0,+} A_+^{1/3} + \bar{\omega}_{0,-} A_-^{1/3}, \quad (\text{A3})$$

$$\bar{\omega}_3 = \bar{\omega}_{0,-} A_+^{1/3} + \bar{\omega}_{0,+} A_-^{1/3}, \quad (\text{A4})$$

where $A_{\pm} = -q/2 \pm \sqrt{\Delta}$, $p = -(\kappa_1^2 + \kappa_2^2 + \nu^2)$, $q = -2\kappa_1\kappa_2\nu \cos \varphi$, $\bar{\omega}_{0,\pm} = (-1 \pm \sqrt{3}i)/2$, and $\Delta = (q/2)^2 + (p/3)^3$ is the discriminant of the solutions. If $\Delta > 0$, there are one real solution and a pair of complex

conjugate solutions. If $\Delta < 0$, there are three different real solutions. If $\Delta = 0$, there are three real solutions but at least two of them are equal.

APPENDIX B: INVERSION SYMMETRIC AND ASYMMETRIC TRIMERIZED LATTICE

The winding number is defined as

$$W = \frac{i}{\pi} \int_{-\pi}^{\pi} \langle u_{\varphi} | \frac{\partial u_{\varphi}}{\partial \varphi} \rangle d\varphi \text{ mod } 2, \quad (\text{B1})$$

where $|u_{\varphi}\rangle$ is the normalized Bloch state [43]. The winding number W is related to the Zak phase γ by $W = \gamma/\pi$. From the calculation results, when $\kappa_1 = \kappa_2 < \nu$, the winding numbers for the upper, central, and lower bands are $W = 1$, $W = 0$, and $W = 1$, respectively. While when $\kappa_1 = \kappa_2 > \nu$, the winding numbers for the three bands are all zero. The winding number W for the general inversion asymmetric chain case where $\kappa_1 \neq \kappa_2 \neq \nu$ is a fraction number and loses its conventional topological meaning.

APPENDIX C: THE ZERO-FREQUENCY EIGENVECTOR

The eigenvector of the zero frequency mode is shown in Fig. 4(a), it is a bulk mode that extends over the entire lattice. Note that the horizontal axis is the resonator index and not the unit-cell index. For example, resonator number 5 is the second resonator of the second unit cell. This eigenvector is denoted by \mathbf{x}_m in the main text. Clearly, in light of its structure, $\delta\mathcal{H}\mathbf{x}_m = \mathbf{0}$ as also explained between Eqs. (3) and (4) above. For the comparison, the eigenvector of the next eigenvalue $\bar{\omega}_{m+1} = \bar{\omega}_1$ is shown in Fig. 4(b), clearly *not* satisfying $\delta\mathcal{H}\mathbf{x}_{m+1} = \mathbf{0}$. This point leads later to the conclusion that the zero-frequency eigenvector is stationary with respect to the disorder Hamiltonian $\delta\mathcal{H}$

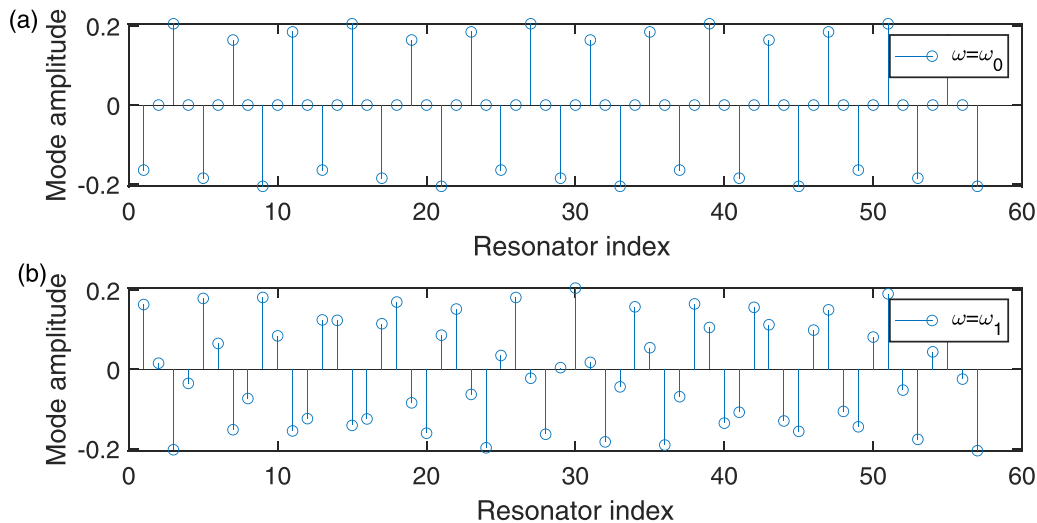


FIG. 4. Typical eigenvectors. (a) Zero-frequency mode. (b) Next mode at ω_1 .

- [1] P. W. Anderson, Absence of diffusion in certain random lattices, *Phys. Rev.* **109**, 1492 (1958).
- [2] M. Segev, Y. Silberberg, and D. Christodoulides, Anderson localization of light, *Nat. Photonics* **7**, 197 (2013).
- [3] D. S. Wiersma, P. Bartolini, A. Lagendijk, and R. Righini, Localization of light in a disordered medium, *Nature (London)* **390**, 671 (1997).
- [4] N. Garcia and A. Z. Genack, Anomalous Photon Diffusion at the Threshold of the Anderson Localization Transition, *Phys. Rev. Lett.* **66**, 1850 (1991).
- [5] C. Ferrari, F. Morichetti, and A. Melloni, Disorder in coupled-resonator optical waveguides, *J. Opt. Soc. Am. B* **26**, 858 (2009).
- [6] L. Martin *et al.*, Anderson localization in optical waveguide arrays with off-diagonal coupling disorder, *Opt. Express* **19**, 13636 (2011).
- [7] S. Mookherjea and A. Oh, Effect of disorder on slow light velocity in optical slow-wave structures, *Opt. Lett.* **32**, 289 (2007).
- [8] C. A. Condat and T. R. Kirkpatrick, Resonant scattering and Anderson localization of acoustic waves, *Phys. Rev. B* **36**, 6782 (1987).
- [9] R. L. Weaver, Anderson localization of ultrasound, *Wave Motion* **12**, 129 (1990).
- [10] J. C. Angel, J. C. Torres Guzman, and A. D. de Anda, Anderson localization of flexural waves in disordered elastic beams, *Sci. Rep.* **9**, 3572 (2019).
- [11] F. J. Dyson, The dynamics of disordered linear chain, *Phys. Rev.* **92**, 1331 (1953).
- [12] H. Schmidt, Disordered one-dimensional crystals, *Phys. Rev.* **105**, 425 (1957).
- [13] C. Domb, On one-dimensional vibrating systems, *Proc. R. Soc. Lond. A* **276**, 418 (1963).
- [14] B. I. Halperin, Green's functions for a particle in a one-dimensional random potential, *Phys. Rev.* **139**, A104 (1965).
- [15] K. Ishii, Localization of eigenstates and transport phenomena in the one-dimensional disordered system, *Prog. Theor. Phys. Suppl.* **53**, 77 (1973).
- [16] S. Alexander, J. Bernasconi, W. R. Schneider, and R. Orbach, Excitation dynamics in random one-dimensional systems, *Rev. Mod. Phys.* **53**, 175 (1981).
- [17] H. Cao, Y. G. Zhao, S. T. Ho, E. W. Seelig, Q. H. Wang, and R. P. H. Chang Random Laser Action in Semiconductor Powder, *Phys. Rev. Lett.* **82**, 2278 (1999).
- [18] B. Abaie, E. Mobini, S. Karbasi, T. Hawkins, J. Ballato, and A. Mafi Random lasing in an Anderson localizing optical fiber, *Light Sci. Appl.* **6**, e17041 (2017).
- [19] J. Li, R.-L. Chu, J. K. Jain, and S.-Q. Shen, Topological Anderson Insulator, *Phys. Rev. Lett.* **102**, 136806 (2009).
- [20] S. Stützer, Y. Plotnik, Y. Lumer, P. Titum, N. H. Lindner, M. Segev, M. C. Rechtsman, and A. Szameit, Photonic topological Anderson insulators, *Nature (London)* **560**, 461 (2018).
- [21] Z. Yu, G. Veronis, Z. Wang, and S. Fan, One-Way Electromagnetic Waveguide Formed at the Interface between a Plasmonic Metal under a Static Magnetic Field and a Photonic Crystal, *Phys. Rev. Lett.* **100**, 023902 (2008).
- [22] Y. Hadad and B. Z. Steinberg, Magnetized Spiral Chains of Plasmonic Ellipsoids for One-Way Optical Waveguides, *Phys. Rev. Lett.* **105**, 233904 (2010).
- [23] Y. Mazor and B. Z. Steinberg Longitudinal chirality, enhanced nonreciprocity, and nanoscale planar one-way plasmonic guiding, *Phys. Rev. B* **86**, 045120 (2012).
- [24] D. L. Sounas, C. Caloz, and A. Alu, Giant non-reciprocity at the subwavelength scale using angular momentum-biased metamaterials, *Nat. Commun.* **4**, 1 (2013).
- [25] Y. Hadad, D. L. Sounas, and A. Alu, Space-time gradient metasurfaces, *Phys. Rev. B* **92**, 100304(R) (2015).
- [26] B. Z. Steinberg, Rotating photonic crystals: A medium for compact optical gyroscopes, *Phys. Rev. E* **71**, 056621 (2005).
- [27] B. Z. Steinberg and A. Boag, Splitting of microcavity degenerate modes in rotating photonic crystals-the miniature optical gyroscopes, *J. Opt. Soc. Am. B* **24**, 142 (2007).
- [28] M. Hafezi, E. A. Demler, M. D. Lukin, and J. M. Taylor, Robust optical delay lines with topological protection, *Nat. Phys.* **7**, 907 (2011).
- [29] Z. Wang, Y. Chong, J. D. Joannopoulos, and M. Soljačić, Observation of unidirectional backscattering-immune topo-

- logical electromagnetic states, *Nature (London)* **461**, 772 (2009).
- [30] L. Lu, J. D. Joannopoulos, and M. Soljačić, Topological photonics, *Nat. Photonics* **8**, 821 (2014).
- [31] A. Khanikaev, R. Fleury, S. Mousavi, and A. Alu, Topologically robust sound propagation in an angular-momentum-biased graphene-like resonator lattice, *Nat. Commun.* **6**, 8260 (2015).
- [32] Y. Mazor and A. Alu, One-way hyperbolic metasurfaces based on synthetic motion, *IEEE Trans. Antennas Propag.* **68**, 1739 (2019).
- [33] Y. Mazor and A. Alu, Nonreciprocal hyperbolic propagation over moving metasurfaces, *Phys. Rev. B* **99**, 045407 (2019).
- [34] E. R. Smith, One-dimensional X-Y model with random coupling constants. I. Thermodynamics, *J. Phys. C: Solid State Phys.* **3**, 1419 (1970).
- [35] G. Theodorou and M. H. Cohen, Extended states in a one-dimensional system with off-diagonal disorder, *Phys. Rev. B* **13**, 4597 (1976).
- [36] T. P. Eggarter and R. Riedinger, Singular behavior of tight-binding chains with off-diagonal disorder, *Phys. Rev. B* **18**, 569 (1978).
- [37] C. M. Soukoulis and E. N. Economou, Off-diagonal disorder in one-dimensional systems, *Phys. Rev. B* **24**, 5698 (1981).
- [38] P. W. Brouwer, C. Mudry, B. D. Simons, and A. Altland, Delocalization in Coupled One-Dimensional Chains, *Phys. Rev. Lett.* **81**, 862 (1998).
- [39] P. W. Brouwer, C. Mudry, and A. Furusaki, Density of States in Coupled Chains with Off-Diagonal Disorder, *Phys. Rev. Lett.* **84**, 2913 (2000).
- [40] F. Zangeneh-Nejad and R. Fleury, Topological analog signal processing, *Nat. Commun.* **10**, 2058 (2019).
- [41] Y. Hadad, J. C. Soric, A. B. Khanikaev, and A. Alù, Self-induced topological protection in nonlinear circuit arrays, *Nat. Electron.* **1**, 178 (2018).
- [42] Y. Hadad, V. Vitelli, and A. Alù, Solitons and propagating domain walls in topological resonator arrays, *ACS Photonics* **4**, 1974 (2017).
- [43] J. Zak, Berry's Phase for Energy Bands in Solids, *Phys. Rev. Lett.* **62**, 2747 (1989).
- [44] T. Ozawa, H. M. Price, A. Amo, N. Goldman, M. Hafezi, L. Lu, M. C. Rechtsman, D. Schuster, J. Simon, O. Zilberberg, and I. Carusotto, Topological photonics, *Rev. Mod. Phys.* **91**, 015006 (2019).
- [45] F. K. Kunst, E. Edvardsson, J. C. Budich, and E. J. Bergholtz, Biorthogonal Bulk-Boundary Correspondence in Non-Hermitian Systems, *Phys. Rev. Lett.* **121**, 026808 (2018).
- [46] V. M. Martinez Alvarez and M. D. Coutinho-Filho, Edge states in trimer lattices, *Phys. Rev. A* **99**, 013833 (2019).
- [47] H. A. Haus, *Waves and Fields in Optoelectronics* (Prentice Hall, New York, 1983).
- [48] C. Yuce, Robust bulk states, *Phys. Lett. A* **383**, 1791 (2019).
- [49] G. W. Stewart and J.-g. Sun, *Matrix Perturbation Theory* (Academic, San Diego, 1990).
- [50] W. Suh, Z. Wang, and S. Fan, Temporal coupled-mode theory and the presence of non-orthogonal modes in lossless multi-mode cavities, *IEEE J. Quantum Electron.* **40**, 1511 (2004).